Criptocrashes

Aleksey Kolokolov
Alliance Manchester Business School,
The University of Manchester
Aleksey.kolokolov@manchester.ac.uk

December 12, 2023

Abstract

This paper proposes a new nonparametric test for detecting short-lived locally explosive trends (drift bursts) in pure-jump processes. The new test is designed specifically to detect intraday flash crashes and gradual jumps in cryptocurrency prices recorded at a high frequency. Empirical analysis shows that drift bursts in bitcoin price occur, on average, every second day. Their economic importance is highlighted by showing that hedge funds holding cryptocurrency in their portfolios are exposed to a risk factor associated with the intensity of bitcoin crashes. On average, hedge funds do not profit from intraday bitcoin crashes and do not hedge against the associated risk.

Keywords: drift burst, pure-jump, flash crash, cryptocurrency, bitcoin, hedge funds

1 Motivation

Cryptocurrency markets are infamous for huge volatility, bubble-like behaviour and abnormal number of flash crashes and dramatic intraday price movements. This paper develops a new econometric methodology for detecting intraday price spikes and crashes from high frequency data and undertakes a systematic analysis of these events. Figure 1 shows two representative examples of the events of interest detected using the new methodology in bitcoin prices. Panel A shows an example of a "flash crash": around 12 : 00 the bitcoin price drops sharply and subsequently recovers in a matter of minutes forming the pattern analogous to the iconic flash crash of May 6, 2010. Panel B represents a positive "gradual jump": the price level changes significantly over a short time interval, however, the price change is not instant (as one expect when the price really jumps), but accumulates continuously forming a short-lived explosive trend.

Figure 1: Examples of drift bursts in bitcoin.

Panel A: a flash crash

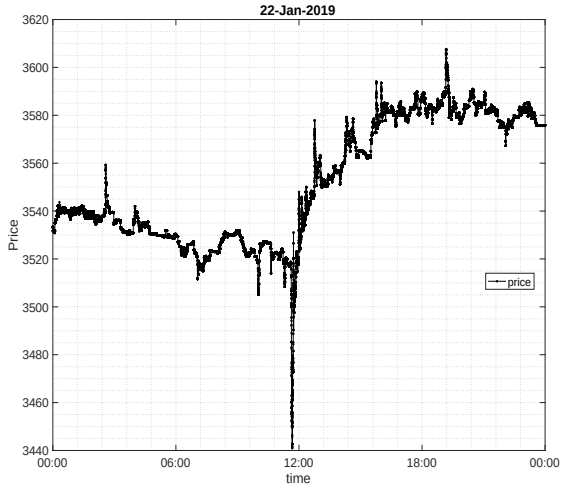

Panel B: a gradual jump

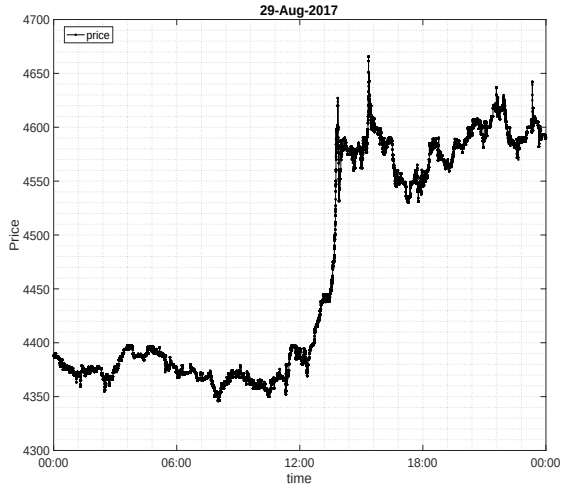

Note. This figure shows two examples of drift bursts detected in bitcoin using the new econometric methodology proposed in the present paper.

Christensen et al. (2022) propose a unified mathematical framework (the drift burst model) incorporating the events as the ones shown in Figure 1 into the classical arbitrage-free continuous-time stochastic volatility models driven by a Brownian motion. However, recent studies (Scaillet et al.,

2020; Kolokolov, 2022) provide strong evidence that the dynamics of the cryptocurrency prices differs substantially from the Brownian stochastic volatility models. In particular, Kolokolov (2022) show that bitcoin price is better described by non-Gaussian pure-jump models without a Brownian motion component. This violates the assumptions of Christensen et al. (2022). Consequently, their nonparametric detection methodology should not be applied to cryptocurrency data.

To overcome the aforementioned difficulty, this paper proposes a new nonparametric test for detecting drift bursts in pure-jump processes. The new methodology remains valid in the classical locally Gaussian models as well. Extensive Monte Carlo experiments show that the size and power of the new test in standard stochastic volatility models driven by a Brownian motion are as good as of the original Christensen et al. (2022) test. In the pure-jump setting, Christensen et al. (2022) test suffers from a loss of power and the new methodology becomes superior.

Application of the new test to high frequency cryptocurrency data reveals a substantial number of drift bursts. Starting from 2018, various kinds of drift bursts occur in bitcoin price roughly every second day on average, while, for example, in the liquid stock prices one can observe roughly 8 similar events in a year as documented by Bellia et al. (2023) using CAC40 stocks traded at Euronext Paris. The majority of drift bursts in bitcoin have a gradual jump form with overshooting: they lead to a shift in the price level, but the original price movement is followed by subsequent partial price reversal. The economic importance of intraday local trends in bitcoin is illustrated by their impact on the performance of hedge funds holding cryptocurrency in their portfolios. By estimating linear factor models for hedge fund returns, we show that, on average, hedge funds profit from positive trends and lose money from negative ones. An average cryptocurrency hedge fund is exposed to the same risks as a long-only bitcoin portfolio: hedge funds are not seem to be crypto-market neutral, they do not diversify bitcoin risks by holding large cryptocurrency portfolios and they are do not implement sophisticated trading strategies to profit during crashes. Consequently, the proposed test for detecting drift bursts can be potentially useful for funds of funds, that might be interested in comparing individual hedge fund returns over particular time intervals (e.g., containing a high number of bitcoin crashes) in order to assess their investment skills and hedging abilities.

The contribution of the present paper is twofold. From the theoretical point of view, the paper

contributes to the broad econometric literature on the inference in pure-jump processes. The majority of studies in this field are dedicated to measuring the jump activity index and volatility or testing for the presence of a Brownian component (Aït-Sahalia and Jacod, 2010; Cont and Mancini, 2011; Jing et al., 2012; Kolokolov, 2022; Woerner, 2003, 2007; Todorov and Tauchen, 2010, 2011; Todorov, 2015; Hounyo and Varneskov, 2017). The present paper is the first study dedicated to the inference on the drift in the class of pure-jump models. Thus, the paper also contributes to the fast growing literature on the inference on the drifts, locally explosive trends and local arbitrage violations from high-frequency data (Christensen et al., 2022; Andersen et al., 2023; Flora and Renó, 2023; Kolokolov et al., 2023; Mancini, 2023).

From the empirical point of view the paper contributes to the recent studies on cryptocurrency markets as well as to the long-established literature on hedge fund performance. Classical questions, such as "do hedge fund really hedge?" and "which factors explain the returns of hedge funds?" are extensively studied for hedge funds investing in conventional assets (Fung and Hsieh, 2001; Titman and Tiu, 2011). The study of cryptocrashes allows to shed light on this questions for the particular group of hedge funds investing in cryptocurrency.

The rest of the paper is organized as follows. Section 2 describes the econometric framework, presents the test statistics and explains the details of its implementation. Section 3 is dedicated to a Monte Carlo study. Real data analysis is conducted in Section 4. Section 5 concludes.

2 Drift bursts in stable noise

2.1 The settings

We consider a filtered probability space $\left(\Omega, \mathscr{F}, (\mathscr{F}_t)_{t\geq 0}, \mathscr{P}\right)$ satisfying usual conditions which supports a log-price process $X = (X_t)_{t\geq 0}$ specified by the assumption below.

Assumption 1. *X is a pure-jump semimartingale evolving as*

$$dX_t = \mu_t\, dt + \sigma_t dS_t, \tag{1}$$

where S is a symmetric α-stable Lévy motion (i.e., $\mathbb{E}\left[e^{i\lambda S_t}\right] = e^{-t|\lambda|^\alpha}$) with Lévy measure $\nu(dz) =$

$B_\alpha |z|^{-(\alpha+1)}\, dz$ *and tail index* $\alpha \in (1,2)$, X_0 *is* $\mathscr{F}_0$*-measurable and independent from* $(S_t)_{t\geq 0}$, $\mu = (\mu_t)_{t\geq 0}$ *is a locally bounded and predictable drift and* $\sigma = (\sigma_t)_{t\geq 0}$ *is an adapted, cádlág, locally bounded stochastic scale.*

Assumption 1 implies that X is a locally stable process. It is a pure-jump analog of a standard formulation for locally Gaussian continuous-time arbitrage-free price processes (a standard locally Gaussian stochastic volatility model with continuous sample paths is obtained by replacing the stable process S with a Brownian motion W). The difference from the classical model is that X is comprised solely of jumps and does not include a continuous martingale component, which is substituted by the infinitely many small jumps in X. The jump activity index of X is equal to the tail index of the driving stable process α. Since $\alpha \in (1,2)$, the jumps of X have infinite variation and the variance of the increments $X_{t+\Delta} - X_t$ computed over short time scales is infinite[1].

The condition $\alpha \in (1,2)$ allows to adopt the drift burst concept of Christensen et al. (2022) to the present pure-jump settings with minor modifications. As μ and σ are locally bounded, for a time instant τ, as $\Delta \to 0$,

$$\int_{\tau-\Delta}^{\tau+\Delta} \mu_t\, dt = O_p(\Delta) \quad \text{and} \quad \int_{\tau-\Delta}^{\tau+\Delta} \sigma_t\, dS_t = O_p(\Delta^{1/\alpha}). \tag{2}$$

Thus, since $\alpha > 1$, over short time intervals the contribution of the drift to the variation of X is negligible relative to the contribution of stochastic scale component. Hence, Assumption 1 describes the "normal times" without drift bursts.

A drift burst occurs in a vicinity of a time point τ (a drift burst time) if, as $\Delta \to 0$,

$$\int_{\tau-\Delta}^{\tau+\Delta} \mu_t\, dt = O_p(\Delta^{\gamma}), \tag{3}$$

with $0 < \gamma < 1/\alpha$. That is, in a neighborhood of τ the drift term diverges prevailing the stochastic scale component.

A stylized example of a drift burst is given by the following semi-parametric specification of the instantaneous drift process:

$$\mu_t^{db} = \frac{a_1}{(\tau - t)^{\alpha(\mu)}} \mathbf{1}_{\{t<\tau\}} + \frac{a_2}{(t - \tau)^{\alpha(\mu)}} \mathbf{1}_{\{t>\tau\}}, \tag{4}$$

[1]The condition $\alpha > 1$ is compatible with real cryptocurrency data used in the empirical application: the average jump activity index estimated by Kolokolov (2022) on five-minute bitcoin data is 1.76.

where a_1 and a_2 are some non-positive (or non-negative) bounded stochastic processes, τ is an $\mathscr{F}_t$-stopping time, $\alpha^{(\mu)}$ is a parameter and $\mathbf{1}_{\{.\}}$ denotes the indicator function. The stopping time τ determines the centre of the drift burst. The parameter $\alpha^{(\mu)} = \gamma - 1$ controls the speed of the explosion. Panel A of Figure 2 shows an example of price trajectory with and without (corresponding to $a_1 = a_2 = 0$) a drift burst. When both a_1 and a_2 are bounded away from zero the drift process specified by equation (4) generates a flash crash similar to the one shown in Panel A of Figure 1. When a_1 is positive and $a_2 = 0$ identically, the parametric model generates a gradual jump similar to the event shown in Panel B of Figure 1. Thus, gradual jumps can be considered as "one-sided flash crashes".

The above example is not unique. Another stylized example of a drift burst having a gradual jump form is the following. Let X' be an auxiliary process satisfying Assumption 1 with μ being locally bounded. Assume that there is a jump $\Delta X'_\tau$ in X' at a time instant τ. Next, define the gradual jump process as:

$$G_t = \Delta X'_\tau \left(1 - \left(1 - \frac{t-\tau}{\tau - \tau'}\right)^\beta\right) \mathbf{1}_{\{t \in [\tau', \tau]\}}, \tag{5}$$

where $\tau' < \tau$ is a stopping time and β is a constant parameter. Then, a process defined as the sum $X_t = X'_t + G_t - \Delta X'_\tau \mathbf{1}_{\{t \geq t\}}$ exhibits a drift burst of a gradual jump form in a vicinity of time τ. Panel B of Figure 2 shows an example of price trajectory with and and without a gradual jump. In this model, X' can be interpreted as a latent fundamental price process which has a large jump at time τ. X stands for the observed price process which accumulates small movements into a level shift at time τ, reflecting the gradually of the market learning.

Other specifications of explosive drifts of different forms can be found in Andersen et al. (2023). In what follows we do not assume a particular parametric form for a drift burst, but propose a nonparametric test for the presence of drift bursts in a pure-jump process defined by Assumption 1.

Remark 1. *The class of pure-jump processes specified by Assumption 1 can be extended in several ways. First, the stable process S in equation (1) can be replaced by a locally stable process, say L, which behaves approximately like a stable process over small time increments only (locally stable processes include, for example, tempered stable processes). Second, the log-price process X may be*

Figure 2: Examples of drift bursts in simulated data.

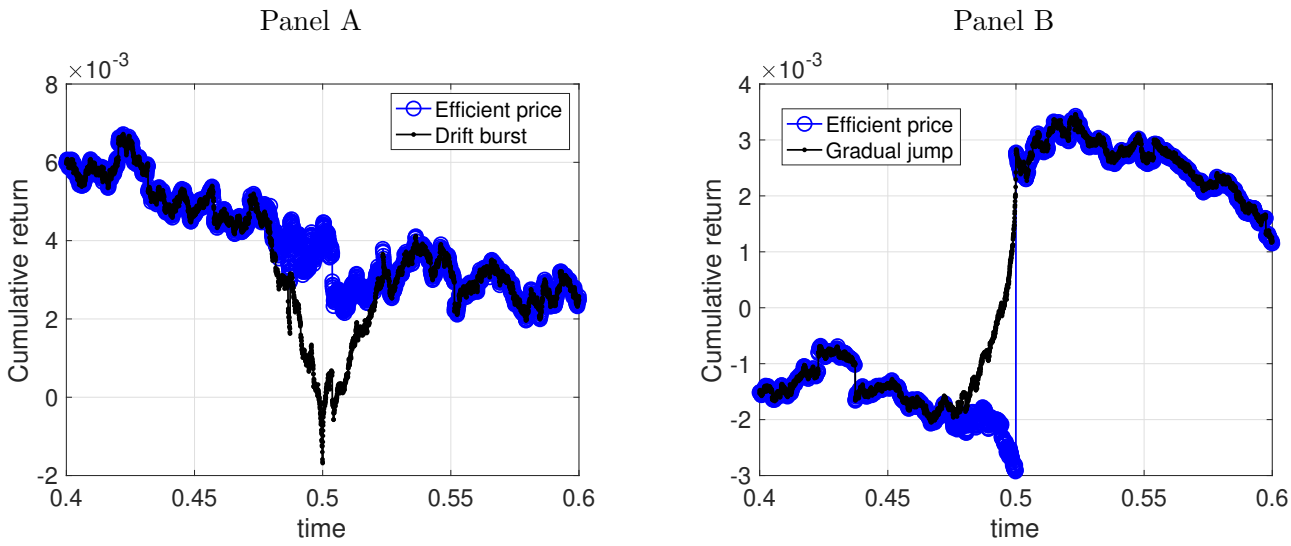

Note. Panel A shows an example of price trajectory with a drift burst generated by model (4). Panel B shows an example of price trajectory with a gradual jump generated by model (5).

allowed to contain "residual" jumps, which are dominated by L over small time scales. Such general setting are considered, for example, in Aït-Sahalia and Jacod (2009), Todorov and Tauchen (2010, 2011), Hounyo and Varneskov (2017) and Kolokolov (2022). The identification theory presented below remains valid under the general setting. However, assuming that the driving force of the log-price in equation (1) is a stable process substantially simplifies the exposition and the mathematical derivations. Hence, Assumption 1 is adopted for convenience and simplicity, but a more general tempered-stable model is used to validate finite sample properties of the proposed test in the Monte Carlo section.

2.2 Identification

The inference is based on a discretized path of X. We assume that X is recorded over a fixed interval $[0, T]$ at times $0 = t_0 < t_1 < \cdots < t_n = T$, where the time increments $\Delta_{i,n} = t_i - t_{i-1}$ are eventually converge to zero. The sampling times are allowed to be non-equispaced, however a certain degree of regularity is required (Assumption 5 in the Appendix). In particular, we assume

that for all i and a sufficiently large n, there exist constants $0 < c < C$, such that

$$c\Delta_n \leq \Delta_{i,n} \leq C\Delta_n, \tag{6}$$

where $\Delta_n = T/n$. In what follows we set $T = 1$ without loss of generality. The high-frequency increments of X over $[t_{i-1}, t_i]$ are denoted by $\Delta_i X = X_{t_i} - X_{t_{i-1}}$.

Nonparametric detection of drift bursts in locally Gaussian models relies on kernel-based local drift and volatility estimators defined respectively as:

$$\mu_t^n = \frac{1}{h_n} \sum_{i=1}^{n} K\left(\frac{t_i - t}{h_n}\right) \Delta_i X \quad \text{and} \quad \sigma_t^n = \sqrt{\frac{1}{h'_n} \sum_{i=1}^{n} K\left(\frac{t_i - t}{h'_n}\right) |\Delta_i X|^2}, \tag{7}$$

where h_n and h'_n are respectively mean and variance bandwidths and K is a kernel function. Bandi (2002) and Kristensen (2010) show that μ_t^n is inconsistent for the drift term but asymptotically normal and unbiased. Using this fact, Christensen et al. (2022) prove that under the absence of a drift burst,

$$t_t^n = \sqrt{\frac{h_n}{K_2}} \frac{\mu_t^n}{\sigma_t^n} \xrightarrow{stably} \mathcal{N}(0, 1), \tag{8}$$

where K_2 is a kernel-dependent constant and $\xrightarrow{stably}$ denotes stable convergence in law. Thus, in locally Gaussian models, the absence of a drift burst in a neighborhood of τ can be rejected when the t-statistics t_τ^n exceeds the corresponding quantile of standard normal distribution.

The above result is not valid for pure-jump models. Recently, Mancini (2023) show that t_t^n does not converge to a Gaussian limit in general pure-jump setting. Intuitively, for locally stable pure-jump semimartingales as in Assumption 1, μ_t^n is not asymptotically Normal due to the nonexistence of the second moment of stable distribution (hence, t_t^n does not converge to normal distribution either) and σ_t^n is unbounded in probability. Consequently, the power of the drift burst test proposed by Christensen et al. (2022) declines with respect to a locally Gaussian case.

To resolve this issue, nonparametric identification of drift bursts in pure-jump stetting relies on tempering high-frequency increments. The increments $\Delta_i X$ are substituted by dampened and normalized counterparts $g\left(\frac{\Delta_i X}{\Delta_n^{1/\alpha}}\right)$, where g is a sufficiently regular tempering function, such that all moments of $g\left(\frac{\Delta_i X}{\Delta_n^{1/\alpha}}\right)$ exist and are finite. The corresponding conditions on g are provided by assumption below.

Assumption 2. *The real valued function g is bounded, infinitely differentiable with bounded derivatives and symmetric around zero with $g(0) = 0$.*

Assumption 2 is satisfied by a wide range of functions. For example, it holds for $g(x) = \Phi(x) - \Phi(0)$, where Φ denotes the cumulative distribution function of standard normal distribution, used in the empirical application. For a given tempering function g, a tempered local drift estimator (an analog of the μ_t^n based on tempered increments) is defined as:

$$\widetilde{\mu}_t^n = \frac{\Delta_n}{h_n} \sum_{i=1}^{n} K\left(\frac{t_{i-1} - t}{h_n}\right) g\left(\frac{\Delta_i X}{\Delta_n^{1/\alpha}}\right). \tag{9}$$

When $T \to \infty$ and $n \to \infty$, a consistent estimator of the drift can be constructed from $\widetilde{\mu}_t^n$ (Mies and Steland, 2019). When T is fixed, the drift can not be estimated consistently. However, $\widetilde{\mu}_t^n$ admits a central limit theorem presented below.

Theorem 2.1. *Assume that X is a semimartingale as defined by Assumption 1, and that Assumptions 2 and 4-6 (stated in the Appendix) are fulfilled. As $n \to \infty$, $h_n \to 0$, $nh_n \to \infty$ and $n^{\frac{2-\alpha}{\alpha}} h_n \to 0$. Then, it holds:*

$$\sqrt{\frac{h_n}{\Delta_n}}\, \widetilde{\mu}_t^n \xrightarrow{stably} \mathcal{N}\left(0, K_2\, \rho_{\sigma_{t-}}^{(\alpha)}\left(g^2\right)\right), \tag{10}$$

where $K_2 = \int_{-\infty}^{0} K^2(x)\, dx$ is a kernel-dependent constant and $\rho_{\sigma_{t-}}^{(\alpha)}(g^2) = \mathbb{E}\left[g\left(\sigma_{t-} S_1\right)^2\right]$, where S_1 denotes standard symmetric α-stable random variable.

Theorem 2.1 shows that tempering high-frequency increments allows to obtain usual Gaussian asymptotics for the functionals of tempered increments even in the pure-jump settings. Rescaling the left-hand side of equation (10) by a suitable estimator of $\sqrt{K_2\, \rho_{\sigma_{t-}}^{(\alpha)}(g^2)}$ provides an asymptotically standard normal test statistic that can identify drift bursts. The test statistics is defined as:

$$\widetilde{t}_t^n = \sqrt{\frac{h_n}{\Delta_n K_2}}\, \frac{\widetilde{\mu}_t^n}{\widetilde{\sigma}_t^n}, \tag{11}$$

where

$$\widetilde{\sigma}_t^n = \sqrt{\frac{\Delta_n}{h_n'} \sum_{i=1}^{n} K\left(\frac{t_{i-1} - t}{h_n'}\right) g^2\left(\frac{\Delta_i X}{\Delta_n^{1/\alpha}}\right)}. \tag{12}$$

Theorem 2.2. *Assume that X is a semimartingale as defined by Assumption 1. Under the assumptions of Theorem 2.1, as $n \to \infty$, it holds:*

$$\widetilde{t}_t^n \xrightarrow{stably} \mathcal{N}(0,1). \tag{13}$$

Theorem 2.2 shows that, in absence of a drift burst, $\widetilde{t}_t^n$ has a limiting standard normal distribution. Thus, the exeedence of $\widetilde{t}_\tau^n$ over a quantile of standard normal distribution indicates the presence of a burst in a vicinity of the stopping time τ.

2.3 Robustness to microstructure noise

This section shows how to modify the test, so it is resistant to a market microstructure noise vastly present at the tick level price data. Assume that instead of directly observing a discretisation of X, the observations are recorded with errors:

$$Z_{t_i} = X_{t_i} + u_{t_i}, \quad i = 0, 1, \ldots, n, \tag{14}$$

where X_{t_i} are discretely sampled from a semimartingale X satisfying Assumption 1 and u_{t_i} are zero-mean random errors specified below.

Assumption 3. *$\{u_{t_i}\}_{i=0}^n$ is a sequence of zero-mean random variables adapted and independent of X. For every i, $\mathbb{E}\left[u_{t_i}^4\right] < \infty$ and the covariance function $\gamma_k = \mathbb{E}\left[u_{t_i} u_{t_{i+k}}\right]$ is finite and independent of i and n for any integer $k \geq 0$. Moreover, there exists an integer $Q > 0$, such that $\gamma_k = 0$ for any $k > Q$.*

Let k_n be a diverging sequence of integers. For a generic stochastic process V, define the pre-averaged increments as:

$$\Delta_i \overline{V} = \sum_{j=1}^{k_n - 1} q_j^n \Delta_{i+j} V, \tag{15}$$

where $q_j^n = q(j/k_n)$, and $q : [0,1] \mapsto \mathbf{R}$ is a continuous and piecewise continuously differentiable function with a piecewise Lipschitz derivative q', $q(0) = q(1) = 0$ and $\int_0^1 q^2(s)\, ds < \infty$.

The noise-robust test statistic is defined as:

$$\overline{t}_t^n = \sqrt{h_n}\, \frac{\overline{\mu}_t^n}{\overline{\sigma}_t^n}, \tag{16}$$

where

$$\overline{\mu}_t^n = \frac{1}{h_n} \sum_{i=1}^{n-k_n+2} K\left(\frac{t_{i-1}-t}{h_n}\right) g\left(\frac{\Delta_{i-1}\overline{Z}}{(n/k_n)^{\frac{1}{\alpha}}}\right), \tag{17}$$

and $\overline{\sigma}_t^n$ is a heteroscedasticity and autocorrelation consistent (HAC)-type estimator of the asymptotic standard deviation of $\overline{\mu}_t^n$ defined as:

$$\overline{\sigma}_t^n = \sqrt{\frac{1}{h'}\left[\left(\sum_{i=1}^{n-k_n+2} K\left(\frac{t_{i-1}-t}{h_n}\right) g\left(\frac{\Delta_{i-1}\overline{Z}}{(n/k_n)^{\frac{1}{\alpha}}}\right)\right)^2 + 2\sum_{L=1}^{L_n} w\left(\frac{L}{L_n}\right) \sum_{i=1}^{n-k_n-L+2} K\left(\frac{t_{i+L-1}-t}{h_n}\right) K\left(\frac{t_{i-1}-t}{h_n}\right) g\left(\frac{\Delta_{i-1}\overline{Z}}{(n/k_n)^{\frac{1}{\alpha}}}\right) g\left(\frac{\Delta_{i+L-1}\overline{Z}}{(n/k_n)^{\frac{1}{\alpha}}}\right)\right]}, \tag{18}$$

where $w : \mathbf{R} \mapsto \mathbf{R}_+$ is a kernel function with $w(0) = 1$ and $\lim_{x\to\infty} w(x) = 0$, and L_n is the lag length that determines the number of autocovariances.

Theorem 2.3. *Assume that Z is defined by equation (14), where X is specified by Assumption 1 and u_{t_i} is specified by Assumption 3. Assumptions 2 and 4-6 (stated in the Appendix) are fulfilled. Assume further that as $n \to \infty$, it holds: $k_n \to \infty$, $L \to \infty$ such that $k_n h_n \to 0$ and $k_n h'_n \to 0$, $h_n k_n^5 n^{\frac{\alpha-2}{\alpha}} \to 0$ and $h'_n k_n^5 n^{\frac{\alpha-2}{\alpha}} \to 0$, $\frac{L_n}{h'_n n} \to 0$. Then, as $n \to \infty$,*

$$\overline{t}_t^n \xrightarrow{stably} \mathcal{N}(0,1). \tag{19}$$

Theorem 2.3 imposes strong conditions on the number of pre-averaged terms: $h_n k_n^5 n^{\frac{\alpha-2}{\alpha}} \to 0$ and $h'_n k_n^5 n^{\frac{\alpha-2}{\alpha}} \to 0$. In practice, these conditions imply that that the number of pre-averaged terms ought to be small. The conditions imposed on L_n are the same as in the Gaussian case.

2.4 Details of implementation

Detection of drift bursts on an interval $[0, T]$ consists of computing our $\overline{t}_t^n$ statistic progressively over a grid of points $0 \leq t_1^* < t_1^* < \cdots < t_m^* \leq T$ partitioning the interval $[0, T]$. To control the family-wise error rate we evaluate the maximum of the absolute values of the test statistic:

$$\overline{t}_\star^n = \max_{t_i^*} \left|\overline{t}_{t_i^*}^n\right|. \tag{20}$$

Then, if $\overline{t}_\star^n$ exceeds its critical value (defined below) we conclude that there is at least one drift bursts in the interval $[0, T]$.

Implementation of this strategy in practice requires the specification of the tuning parameters for computing $\overline{t}^n_{t^*_i}$ in each point of the grid and of the critical value for $\overline{t}^n_\star$. Since the test statistics $\overline{t}^n_{t^*_i}$ have asymptotic standard normal distribution, the solution to the later problem does not differ from the Gaussian case and it is borrowed from Christensen et al. (2022). In particular, we approximate the time series of the test statistics $\overline{t}^n_{t^*_1}, \overline{t}^n_{t^*_2}, \ldots, \overline{t}^n_{t^*_m}$ by an $AR(1)$ process, estimate the autoregressive parameter using conditional maximum likelihood and simulate 100,000,000 Monte Carlo replications of the $AR(1)$ process. Then, q-% the data-driven critical value for $\overline{t}^n_\star$ is computed as the q-% quantile of the maximums of the absolute values of the simulated $AR(1)$ processes.

For each $\overline{t}^n_{t^*_i}$ from the grid, we choose the tempering function to be $g(x) = \Phi(x) - \Phi(0)$, where $\Phi(x)$ denotes the cdf of standard normal distribution. This particular tempering function is adopted as a similar function is successfully used by Mies and Steland (2019) for the drift estimation under long-span asymptotic. For the choice of the remaining tuning parameters we again follow the suggestions of Christensen et al. (2022). We set $k_n = 3$ and calculate the drift burst test statistic on a regular 30-second grid and only include values that are preceded by a price change (stale prices corresponding to zero returns are removed). The bandwidth for the spot volatility estimation is specified as five times the bandwith for the drift $h'_n = 5h_n$, we use Parzen kernel and $L_n = 2(k_n + 1) + 10$ lags for the HAC-correction and left-sided exponential kernel $K(x) = exp(-|x|)$, for $x \leq 0.23$. For the estimation of the drift we use a large bandwidth of 20 minutes.

Finally, the computation of $\overline{t}^n_{t^*_i}$ requires scaling the pre-averaged returns by a factor $(n/k_n)^{\frac{1}{\alpha}}$, where α is an unknown jump activity index. From the proof of Theorem 2.3 it is clear that the scaling factor can be replaced with another sequence converging with the same rate. Therefore, to avoid the estimation of α in practice we replace the tempered local drift estimator with a self-normalized statistics:

$$\overline{\mu}^n_t = \frac{1}{h_n} \sum_{i=1}^{n-k_n+2} K\left(\frac{t_{i-1} - t}{h_n}\right) g\left(\frac{\Delta_{i-1}\overline{Z}}{\theta_n}\right), \tag{21}$$

where $\theta_n = \frac{\frac{1}{n-k_n+2} \sum_{i=1}^{n-k_n+2} \left|\Delta_{i-1}\overline{Z}\right|}{c_\theta}$, with c_θ being a constant. c_θ can be interpreted similarly to the constant in the definition of the adaptive threshold used by Corsi et al. (2010): it controls how large should be the increment $\left|\Delta_{i-1}\overline{Z}\right|$ relative to the average value to be truncated by the function g. We set $c_\theta = 0.2$, which guarantees that for the increments, which are more than 15 times larger

than the average, we have $\left|g\left(\frac{\Delta_{i-1}\overline{Z}}{\theta_n}\right)\right| \approx 0.5 = g(\infty)$, so the extremely large jumps are replaced by a finite value. The local volatility estimator is adjusted in a similar way.

3 Simulation study

In this section we investigate the finite-sample size and power of the proposed test by Monte Carlo simulations. The overall goal is to compare the new drift burst test with the original test developed for Brownian models by Christensen et al. (2022). Therefore we adopt the same simulation setting as in their paper extending it further by replacing Brownian motion with pure-jump processes.

The driftless "efficient" log-price process X evolves as:

$$\begin{aligned} dX_t &= \gamma^{(\alpha)}\,\sigma_t\,dL_t^{(\alpha)}, \\ d\sigma_t^2 &= \kappa(\theta-\sigma_t^2)\,dt + \xi\sigma_t dB_t, \quad t\in[0,1], \end{aligned} \tag{22}$$

where B is a standard Brownian motion and $L^{(\alpha)}$ is either a locally stable processes (when $\alpha<2$) or a standard Brownian motion (when $\alpha=2$), such that $\mathbb{E}\left[dL_t^{(2)}\,dB_t\right]=\rho$. When $\alpha<2$, the pure-jump process $L^{(\alpha)}$ is specified as in Kolokolov (2022): it is a mixture of tempered stable processes with the Lévy measure $\nu_L(x)=e^{-\lambda|x|}\left(\frac{A_0}{|x|^{\alpha+1}}+\frac{A_1}{|x|^{\alpha/3+1}}\right)$.

We consider different values of the jump activity index α ranging in the interval $(1,2]$ and choose other parameters as in Christensen et al. (2022) and Kolokolov (2022). The annualized volatility parameters are $(\kappa,\theta,\xi,\rho)=\left(5,0.0225,0.4,-\sqrt{0.5}\right)$. For each value of α, $\lambda=0.25$ and A_0 and A_1 are such that $A_0\int_{\mathbf{R}}|x|^{1-\alpha}\,e^{-\lambda|x|}\,dx=1$ and $A_1\int_{\mathbf{R}}|x|^{1-\alpha}\,e^{-\lambda|x|}\,dx=0.2$. Next, for each of the simulated paths, the constants $\gamma^{(\alpha)}$ are calibrated to guarantee that the quadratic variation of X is the same for different values of α and $\gamma^{(2)}=1$, so the relative contribution of the drift burst is the same across considered levels of jump activity. A total of 1000 repetitions is generated via an Euler discretization. In each simulation, $n=23400$ and σ_t^2 is initiated at random from its stationary law.

To asses the power of the test under alternative we add drift and volatility bursts components (although, the presence of volatility bursts is not considered in the theory, they are added to intricate

the Monte Carlo experiments) to the log-price process X, so the observed process becomes:

$$\widetilde{X}_t = X_t + \int_0^t \mu_s^{db}\, ds + \int_0^t \sigma_s^{vb}\, dL_s^{(\alpha)}, \tag{23}$$

where the parametric form of the drift and volatility bursts are respectively:

$$\mu_t^{db} = a\frac{sign(t-\tau)}{|\tau - t|^{\alpha^{(\mu)}}}, \quad \sigma_s^{vb} = b\frac{\sqrt{\theta}}{|\tau - t|^{\beta}}. \tag{24}$$

We set $\tau = 0.5$, so the the price experiences a short-lived flash crash at the centre of the simulated trading day. We consider small, medium and large drift bursts corresponding to three different explosion rates $\alpha^{(\mu)} \in \{0.55, 0.65, 0.75\}$ and $a = 3$. The parameters of the volatility bursts are $b = 0.15$ and $\beta = 0.5$ which guarantee satisfactory identification of the drift burst in the Gaussian case according to the simulations in Christensen et al. (2022).

Table 1 reports the number of rejections of the absence of a drift burst in the model defined by equation (22) for different levels of the jump activity α. Panel A reports the rejections for the Christensen et al. (2022) test. Panel B reports the number of rejections for the new test. First, the table shows that in the standard Gaussian case (the bottom rows of Panels A and B) the performances of the two tests are not significantly different. For example, with the 95% confidence level, medium and large drift burst are detected by the original test in respectively 46.3% and 84.2% of the simulations; the new test detects these drift bursts in respectively 45.4% and 86.3% of the simulations. However, the power of the new test in significantly larger than the power of the original test for the pure-jump setting. For example, when jump activity $\alpha = 1.5$, small, medium and large drift bursts are detected (with the 95% confidence level) by the original tests in respectively 37.8%, 69.7% and 90% of the simulations, while the new test detects them in respectively 68.0%, 94.2% and 99.5% of the simulations. Second, Table 1 shows that the smaller the jump activity index the easier it is to detect a drift bursts. Intuitively this result can be explain as follows. The quadratic variation of a pure-jump process is equal to the sum of squared jumps. When the jump activity index is small, there are just a few very large jumps, which account for the major part of the quadratic variation. The increments of X not containing the largest jumps are relatively small. Hence, the contribution of the (exploding) drift to this increments is relatively larger and can be easier captured by the test statistics.

Table 1: Size and power of drift burst t-statistics.

		$\mathscr{P}\left(t_m^\star > q_{0.950}\right)$				$\mathscr{P}\left(t_m^\star > q_{0.990}\right)$				$\mathscr{P}\left(t_m^\star > q_{0.995}\right)$			
		Size	**Power:** $\alpha^{(\mu)} =$			**Size**	**Power:** $\alpha^{(\mu)} =$			**Size**	**Power:** $\alpha^{(\mu)} =$		
		$\mu^{db} = 0$	0.55	0.65	0.75	$\mu^{db} = 0$	0.55	0.65	0.75	$\mu^{db} = 0$	0.55	0.65	0.75
Panel A:		Christensen, Oomen, Renó (2020) test											
$\alpha =$	1.1	0.017	0.583	0.801	0.923	0.009	0.518	0.744	0.888	0.008	0.496	0.718	0.876
	1.2	0.009	0.521	0.784	0.949	0.006	0.452	0.716	0.908	0.005	0.427	0.690	0.890
	1.3	0.008	0.456	0.757	0.911	0.003	0.383	0.684	0.866	0.003	0.355	0.647	0.845
	1.4	0.005	0.409	0.706	0.919	0.002	0.312	0.607	0.869	0.002	0.290	0.565	0.833
	1.5	0.007	0.378	0.697	0.900	0.003	0.293	0.599	0.841	0.003	0.267	0.549	0.808
	1.6	0.011	0.353	0.633	0.894	0.002	0.253	0.523	0.815	0.001	0.222	0.491	0.776
	1.7	0.014	0.286	0.621	0.897	0.003	0.190	0.471	0.812	0.002	0.162	0.421	0.764
	1.8	0.027	0.243	0.541	0.876	0.008	0.154	0.397	0.777	0.003	0.131	0.339	0.719
	1.9	0.022	0.208	0.498	0.852	0.006	0.108	0.359	0.750	0.001	0.078	0.310	0.693
	2	0.043	0.177	0.463	0.842	0.003	0.089	0.287	0.697	0.003	0.059	0.234	0.634
Panel B:			New test										
$\alpha =$	1.1	0.045	0.961	0.998	1.000	0.032	0.927	0.994	1.000	0.028	0.913	0.993	1.000
	1.2	0.027	0.908	0.994	1.000	0.017	0.865	0.991	1.000	0.016	0.847	0.987	1.000
	1.3	0.028	0.847	0.988	1.000	0.017	0.777	0.979	1.000	0.012	0.751	0.972	0.998
	1.4	0.017	0.783	0.973	0.999	0.007	0.686	0.951	0.997	0.006	0.641	0.936	0.995
	1.5	0.021	0.680	0.942	0.995	0.007	0.566	0.892	0.988	0.005	0.531	0.859	0.986
	1.6	0.029	0.559	0.871	0.993	0.010	0.440	0.800	0.983	0.006	0.394	0.748	0.968
	1.7	0.022	0.427	0.820	0.989	0.004	0.309	0.703	0.964	0.003	0.279	0.650	0.945
	1.8	0.038	0.326	0.681	0.964	0.004	0.224	0.550	0.925	0.002	0.192	0.492	0.885
	1.9	0.028	0.229	0.552	0.918	0.007	0.126	0.419	0.850	0.004	0.097	0.368	0.806
	2	0.038	0.171	0.454	0.863	0.003	0.075	0.285	0.749	0.002	0.050	0.231	0.681

Note. The table reports the number of rejections of the absence of a drift burst in the model defined by equation (22) for different levels of jump activity α. Panel A reports the rejections for the Christensen, Oomen, Renó (2020) test. Panel B reports the number of rejections for the new test proposed in the present paper.

Figure 3 shows the correlation between the original and the new test statistics in Gaussian (Panel A) and pure-jump (Panel B) settings. Under the presence of the Brownian motion the two tests are highly correlated and most of the time they detect drift bursts in the same simulated trajectories of X. Panel B shows that in the pure-jump case (with jump activity index $\alpha = 1.5$) the two test statistics remain correlated, but the scatter plot substantially deviates from the 45 degree line indicating larger power of the new test. The relative loss of power for the original test is consistent with the theoretical intuition: since in the pure-jump settings the standard local volatility estimator in the denominator of the test statistics is unbounded in probability, the value of the original test statistic decreases.

Figure 3: Original v.s. new drift burst tests.

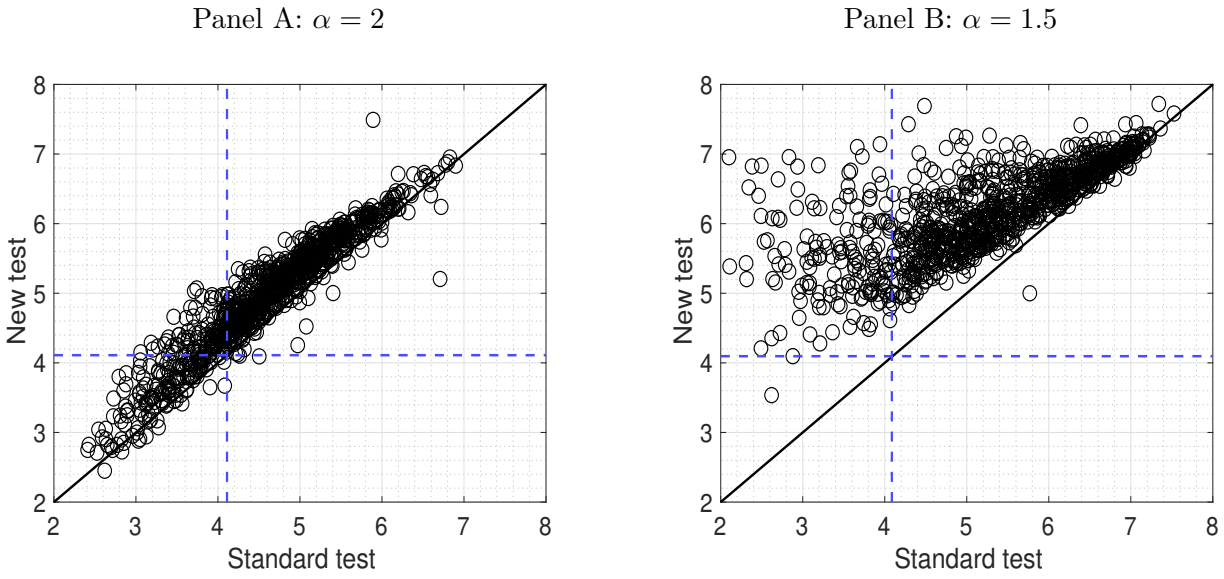

Note. This figure shows the scatter plot of the original drift burst statistics of Christensen, Oomen, Renó (2022) against the new test statistics in Gaussian case (Panel A) and pure-jump case with $\alpha = 1.5$ (Panel B). The blue dashed lines represents average 99% critical values.

Overall, the Mote Carlo experiments show that the newly proposed test is more suitable for detecting drift bursts in cryptocurrency prices. Even if the jump activity of an underling cryptocurrency price varies over time or approaches the value of 2, application of the new methodology allows safely detecting drift bursts without risking the test power and without any visible size distortion.

4 Application to real data

4.1 Bitcoin crashes

We consider a time series of tick-by-tick bitcoin prices traded at Kraken recorded from January 1, 2017 to April 19, 2022. In total we obtain 1934 trading days with 24 hours in each. The data are available from *www.bitcoincharts.com*. In order to detect drift bursts in bitcoin prices the noise-robust test statistic $\bar{t}_t^n$ is computed for every trading day on a grid of equispaced time points distant by 30-seconds intervals. The tuning parameters are set as explained in Section 2.4. In order to be able to detect drift bursts occurring during the same trading day the maximum test statistic $\bar{t}_\star^n$ defined by equation (20) is calculated every hour. Each detected drift burst is classified as being positive or negative based on the sign of the test statistics.

Table 2 reports the number of positive and negative drift bursts detected in bitcoin price and average of 5, 10- and 30-minute returns before and after the drift bursts peaks. On average, a drift burst with any sign occurs in roughly 42% of trading days. Panel A of Figure 4 illustrates the temporal distribution of drift burst across trading days and trading hour during the day. In 2017 (when bitcoin market was not yet very developed and relatively illiquid) bitcoin crashes occur relatively less frequent than in the later years. After 2018 drift bursts occur on average every second day. They are scattered nearly uniformly across the years and the time of the day, without a clear pattern, which might be associated with a specific time of the day. Several drift bursts frequently occur on the same day. The frequency of positive and negative events is roughly the same.

Panel B of Figure 4 shows the scatter plot of pre- and post-drift burst returns. We observe that some of drift bursts can be associated with subsequent partial price reversals (the reversals are not always statistically significant). This result resembles the findings of Christensen et al. (2022) based on the analysis of drift bursts in different future contracts. In order to test the significance of the price reversals, for each of the detected event, the proposed test is applied in reverse time. Panels B and C of Table 2 report the number of detected crashes respectively with subsequent significant reversals and without them. The majority of the crashes – roughly 83% for positive

Table 2: Drift bursts detected in bitcoin prices.

	#	$R_5^{(-)}$	$R_5^{(+)}$	$R_{10}^{(-)}$	$R_{10}^{(+)}$	$R_{30}^{(-)}$	$R_{30}^{(+)}$
	Panel A: All events						
positive	428	0.016	−0.003	0.020	−0.003	0.024	−0.003
		(0.013)	(0.008)	(0.016)	(0.009)	(0.018)	(0.012)
negative	400	−0.021	0.006	−0.026	0.006	−0.032	0.006
		(0.020)	(0.015)	(0.027)	(0.017)	(0.032)	(0.023)
	Panel B: With significant reversals (gradual jumps with overshooting)						
positive	71	0.016	−0.008	0.019	−0.010	0.024	−0.016
		(0.016)	(0.010)	(0.018)	(0.011)	(0.021)	(0.015)
negative	96	−0.025	0.014	−0.031	0.017	−0.039	0.023
		(0.024)	(0.019)	(0.031)	(0.023)	(0.043)	(0.035)
	Panel C: Without significant reversals (gradual jumps)						
positive	357	0.015	−0.003	0.020	−0.002	0.025	−0.001
		(0.013)	(0.007)	(0.015)	(0.008)	(0.017)	(0.010)
negative	304	−0.020	0.003	−0.024	0.003	−0.030	0.001
		(0.019)	(0.012)	(0.025)	(0.014)	(0.027)	(0.015)

Note. The table reports the number of positive and negative drift bursts detected in bitcoin prices for the period from January 1, 2017 to April 19, 2022. The second column reports the number of detected events. The other columns report the average 5, 10- and 30 minute returns before ($R_5^{(-)}$,$R_{10}^{(-)}$,$R_{30}^{(-)}$) and after ($R_5^{(+)}$,$R_{10}^{(+)}$,$R_{30}^{(+)}$) the peak of drift bursts and their standard deviations (in parenthesis).

and 75% for negative drift bursts – have gradual jump form: they are not followed by significant price reversals. Negative drift bursts tend to revert more relative to positive ones. The price drops observed during the crashes with reversals are slightly larger than during gradual jumps: for example, average 10-minute return during a price crash associated with subsequent price recovery is -3.1%, while it is -2.5% for the crashes without significant reversals.

Figure 5 presents average shapes of detected drift bursts. It displays average (across detected events of different kinds) cumulative log-returns in one hour interval surrounding drift burst instant.

4.2 An economic lens: impact on hedge fund performance

This section study how drift bursts in bitcoin impact the performance of cryptocurrency investors. While a long-only bitcoin investors profit from positive gradual jumps and lose from negative ones, sophisticated investors, for example, hedge funds, may benefit from both kinds of bursts (or at

Figure 4: Temporal distribution and reversion of drift bursts.

Panel A

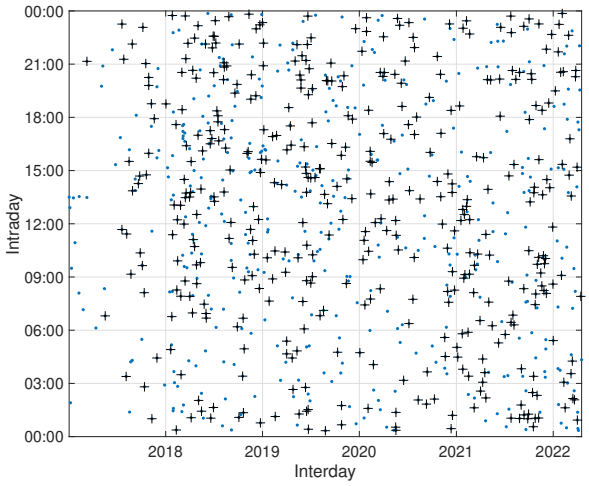

Panel B

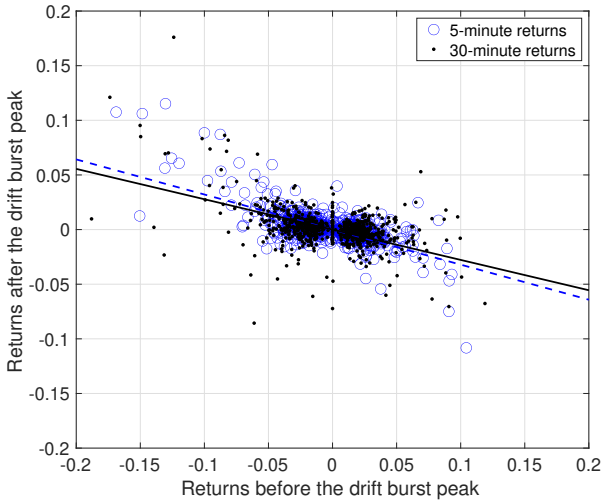

Note. Panel A shows the distribution the drift bursts instants across days and time of a day. Positive drift bursts are labeled with +. Panel B shows the scatter plot of 5 and 30 minutes pre- and post-drift burst returns.

least annihilate the risk caused by bitcoin crashes) by proper market timing, short selling, trend following strategies and holding well-diversified portfolios of various cryptocurrencies. To test the later claim we estimate various multi-factor models for the Barclay Cryptocurrency Traders Index (BCTI), which measures the average performance of hedge funds holding cryptocurrency in their portfolios. Along with standard factors typically used to explain hedge fund returns (Fung and Hsieh, 2001) we add new ones measuring the intensity of drift bursts in bitcoin. The data for BCTI are available on monthly level from January 2018 to May 2021 from the Barclay Hedge database.

We consider several linear factor models for BCTI specified as:

$$R_t = \alpha + \beta_1 \lambda_t^+ + \beta_2 \lambda_t^- + \beta' \text{Controls}_t + \varepsilon_t, \tag{25}$$

where R_t is the value of BCTI on month t, λ_t^+ and λ_t^- denote the monthly intensity of respectively positive and negative drift bursts (measured by the number of detected bursts in each month), Controls_t is a vector of standard factors used to explain hedge fund returns and ε_t is a stochastic error term. First, the model is estimated without control variables. Next, controls are added into the regression. Finally, we distinguish between gradual jumps with and without subsequent price

Figure 5: Average shapes of the drift bursts.

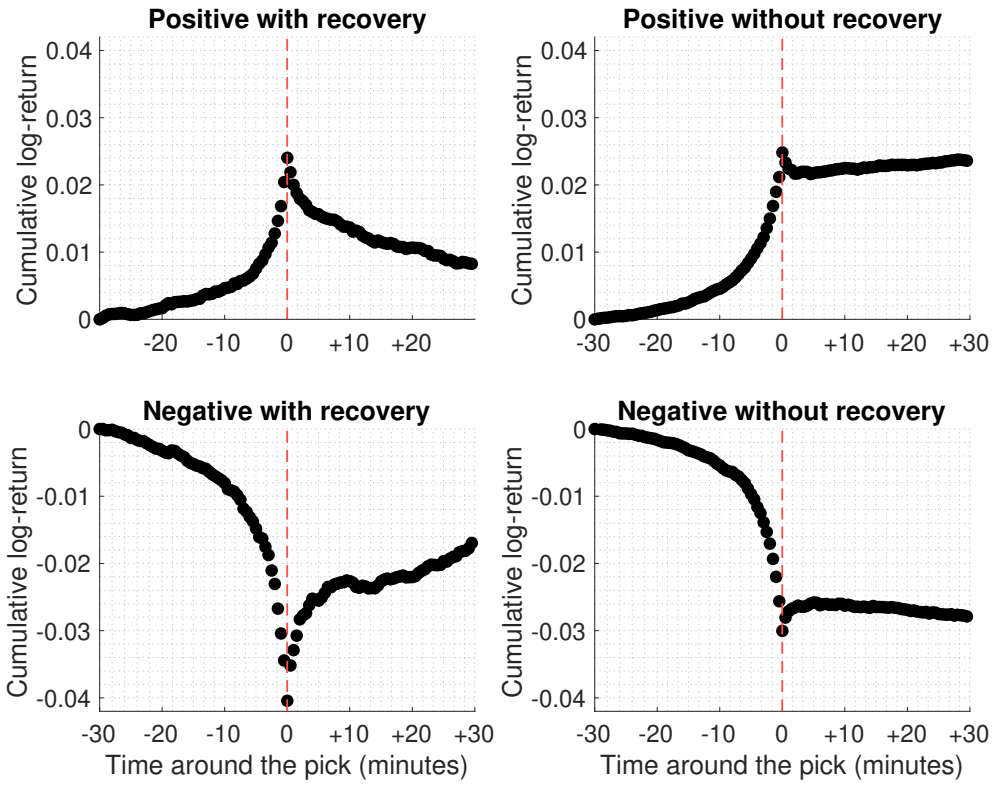

Note. Average positive (left panel) and negative (right panel) drift bursts in bitcoin with and without significant price overshooting and subsequent price reversals.

reversals by replacing λ_t^+ and λ_t^- in the regression equation by the intensities of the corresponding events.

Table 3 presents the estimates of the regression coefficients from different specifications of the model (25). The intensities of both positive and negative drift bursts are highly significant. They explain 41.8% of the variation of BCTI, while standard hedge-fund factors (Controls_t) taken alone capture only 17.8% of the total variation. The partial effect of positive gradual jumps on BCTI is positive and the effect of negative ones is negative. Thus, on average, hedge funds do not profit from intraday bitcoin crashes and they do not hedge against the associated risk. Splitting drift burst into the events with and without price reversals shows that the above-mentioned effect is due to the gradual jumps without overshooting. The intensity of the reverting events is not significant.

Table 3: Impact on hedge fund returns.

const	5.689	3.572	12.108	11.363	0.554
	(0.885)	(0.511)	(1.538)	(1.301)	(0.194)
λ_t^+	2.604***		1.809***		
	(3.951)		(2.615)		
λ_t^-	−3.146***		−3.217***		
	(−4.706)		(−4.004)		
$\lambda_t^{+,(1)}$		−0.279		−0.330	
		(−0.170)		(−0.190)	
$\lambda_t^{+,(0)}$		2.842***		2.101***	
		(4.472)		(3.018)	
$\lambda_t^{-,(1)}$		−0.191		−1.235	
		(−0.129)		(−0.758)	
$\lambda_t^{-,(0)}$		−3.387***		−3.540***	
		(−5.266)		(−4.292)	
Mkt_RF			−0.603	−0.535	−0.689
			(−0.997)	(−0.897)	(−0.949)
SMB			2.087***	1.776**	2.772***
			(2.735)	(2.317)	(3.019)
PTFSBD			0.080	0.065	0.125
			(0.948)	(0.766)	(1.201)
PTFSFX			−0.141	−0.130	−0.053
			(−1.094)	(−0.993)	(−0.339)
PTFSCOM			0.158	0.086	0.490**
			(0.869)	(0.444)	(2.370)
PTFSIR			0.053	0.074	−0.212
			(0.350)	(0.495)	(−1.277)
PTFSSTK			−0.155	−0.161	−0.127
			(−1.143)	(−1.159)	(−0.776)
BondMkt			0.003	0.003	−0.009
			(0.024)	(0.022)	(−0.063)
CreditSpread			0.009	0.044	−0.114
			(0.070)	(0.338)	(−0.719)
R^2	0.446	0.529	0.612	0.653	0.359
$\overline{R}^2$	0.418	0.478	0.469	0.492	0.178

Note. The table reports OLS estimates of the regression coefficients from model (25) with different sets of regressors. t-statistics are in parenthesis. Coefficients significant at 95, 99 and 99.9% level are indicated respectively with *, ** and ***. The regressors are following: λ_t^+ and λ_t^- are the intensities of respectively positive and negative drift bursts, $\lambda_t^{+,(1)}$, $\lambda_t^{+,(0)}$ and $\lambda_t^{-,(1)}$, $\lambda_t^{-,(0)}$ are respectively the intensities of respectively positive and negative drift bursts with and without subsequent price recovery. Mkt_RF, SMB, BondMkt, CreditSpread denote respectively market, size, bond market and credit risk factors. PTFSBD, PTFSFX, PTFSIR, PTFSSTK are respectively risk factors computed by Fung and Hsieh (2001).

The above results complement the findings on hedge funds investing in conventional assets. Hedge fund returns can be divided into two components: a passive component that tracks an index or a passive portfolio, and an active component uncorrelated with the first one. Titman and Tiu (2011) show that most hedge funds are not market neutral and they are exposed to systematic risk factors. They also find that individual hedge funds that are least exposed to systematic factors have higher Sharpe ratios, higher information ratios, and higher alphas. Our results show that the intensity of drift bursts in bitcoin forms a systematic risk factor for the hedge funds investing in cryptocurrency. The study of the effect of this new systematic factor on individual hedge funds may be an interesting avenue for future research.

5 Conclusion

This paper proposed a novel nonparametric test for detecting intraday price spikes and crashes using the high-frequency data. The test is designed specifically for pure-jump processes, with cryptocurrency prices being one of the prominent examples. The amount of crashes detected in cryptocurrency prices is much larger than in conventional assets. Drift bursts in bitcoin price occur on average every second day with no particular pattern with respect to time of a day. Sophisticated market participants, such as hedge funds, are exposed to systematic risk associated with the intensity of crashes in bitcoin price.

References

Aït-Sahalia, Y., Jacod, J., 2009. Estimating the degree of activity of jumps in high frequency financial data. Annals of Statistics 37, 2202–2244.

Aït-Sahalia, Y., Jacod, J., 2010. Is Brownian motion necessary to model high frequency data? Annals of Statistics 38, 3093–3128.

Andersen, T.G., Li, Y., Todorov, V., Zhou, B., 2023. Volatility measurement with pockets of extreme return persistence. Journal of Econometrics 237, 105048.

Bandi, F.M., 2002. Short-term interest rate dynamics: a spatial approach. Journal of Financial Economics 65, 73–110.

Bellia, M., Christensen, K., Kolokolov, A., Pelizzon, L., Reno, R., 2023. Do designated market makers provide liquidity during extreme price movements? Working paper.

Christensen, K., Oomen, R., Renó, R., 2022. The drift burst hypothesis. Journal of Econometrics 227, 461–497.

Cont, R., Mancini, C., 2011. Nonparametric tests for pathwise properties of semimartingales. Bernoulli 17, 781–813.

Corsi, F., Pirino, D., Renó, R., 2010. Threshold bipower variation and the impact of jumps on volatility forecasting. Journal of Econometrics 159, 276–288.

Flora, M., Renó, R., 2023. V-shapes. Working paper.

Fung, W., Hsieh, D.A., 2001. The risk in hedge fund strategies: Theory and evidence from trend followers. The Review of Financial Studies 14, 313–341.

Hounyo, U., Varneskov, R.T., 2017. A local stable bootstrap for power variations of pure-jump semimartingales and activity index estimation. Journal of Econometrics 198, 10–28.

Jacod, J., Protter, P., 2012. Discretization of Processes. Springer-Verlag.

Jing, B.Y., Kong, X.B., Liu, Z., 2012. Modeling high-frequency financial data by pure jump processes. The Annals of Statistics 40, 759–784.

Kolokolov, A., 2022. Estimating jump activity using multipower variation. Journal of Business & Economic Statistics 40, 128–140.

Kolokolov, A., Renó, R., Zoi, P., 2023. Bumvu estimators. Working paper.

Kristensen, D., 2010. Nonparametric Filtering of the Realized Spot Volatility: A Kernel-Based Approach. Econometric Theory 26, 60–93.

Mancini, C., 2023. Drift burst test statistic in the presence of infinite variation jumps. Stochastic Processes and their Applications 163, 535–591.

Mancini, C., Mattiussi, V., R, R., 2015. Spot volatility estimation using delta sequences. Finance & Stochastics 19, 261–293.

Mies, F., Steland, A., 2019. Nonparametric gaussian inference for stable processes. Statistical Inference for Stochastic Processes 22, 525–555.

Rosinski, J., Woyczynski, W., 1985. Moment inequalities for real and vector p-stable stochastic integrals., in: Probability in Banach spaces, Springer, Berlin. pp. 369–386.

Scaillet, O., Treccani, A., Trevisan, C., 2020. High-frequency jump analysis of the bitcoin market. Journal of Financial Econometrics 18, 209–232.

Titman, S., Tiu, C., 2011. Do the best hedge funds hedge? The Review of Financial Studies 24, 123–168.

Todorov, V., 2015. Jump activity estimation for pure-jump semimartingales via self-normalized statistics. Annals of Statistics 43, 1831–1864.

Todorov, V., Tauchen, G., 2010. Activity signature functions for high-frequency data analysis. Journal of Econometrics 154, 125–138.

Todorov, V., Tauchen, G., 2011. Limit theorems for power variations of pure-jump processes with application to activity estimation. Annals of Applied Probability 21, 546–588.

Woerner, J., 2003. Variational sums and power variation: A unifying approach to model selection and estimation in semimartingale models. Statistics and Decisions 21, 47–68.

Woerner, J., 2007. Inference in Lévy-type stochastic volatility models. Advances in Applied Probability 39, 531–549.

A Mathematical appendix

Below $C > 0$ denotes a generic positive constant which changes from line to line.

A.1 Assumptions and auxiliary results

This section summarise the technical assumptions and their implications repeatedly used in the proofs.

Assumption 4. *Fix $t \in [0, T]$. Assume there exists a $\Gamma > 0$ and a sequence $(\tau_m)_{m\geq 1}$ of $\mathscr{F}_t$-stopping times with $\tau_m \to \infty$ and constants $C_t^{(m)}$, such that for all m,*

$$\mathbb{E}\left[|\mu_u - \mu_s|^2 + |\sigma_u - \sigma_s|^2 \,\middle|\, \mathscr{F}_s\right] \leq C_t^{(m)} |u - s|^\Gamma , \tag{26}$$

for all all $0 \leq s \leq u \leq T \wedge \tau_m$.

Assumption 4 holds for a large class of stochastic processes. For example, due to the Burkholder-Davis-Gundy inequality it allows σ to be a Brownian semimartingale plus jumps. By a localization procedure as in Jacod and Protter (2012, Section 4.4.1), in all the following proofs we assume without loss of generality that μ and σ are bounded. In that case, Assumption 4 implies that, for any $r \geq 2$,

$$\mathbb{E}\left[|\sigma_u - \sigma_s|^r \mid \mathscr{F}_s\right] \leq C |u - s|^\Gamma . \tag{27}$$

For $r = 1$, due to Jensens's inequality,

$$\mathbb{E}\left[|\sigma_u^\alpha - \sigma_s^\alpha| \mid \mathscr{F}_s\right] \leq C |u - s|^{\Gamma/2} , \tag{28}$$

for any $\alpha \in [1, 2]$.

Assumption 5. *$\{t_i\}_{i=0}^n$ is a deterministic sequence. Let $\Delta_n^- = \min_{1,\ldots,n} \Delta_{i,n}$ and $\Delta_n^+ = \max_{1,\ldots,n} \Delta_{i,n}$ and assume that, for a sufficiently large n, there exists positive constants c and C, such that*

$$c\Delta_n \leq \Delta_n^- \leq \Delta_n^+ \leq C\Delta_n, \tag{29}$$

where $\Delta_n = T/n$. Moreover, denoting the "quadratic variation of time up to t" as $H(t) = \lim_{n\to\infty} H_n(t)$, where $H_n(t) = \frac{1}{\Delta_n} \sum_{t_i \leq t} (\Delta_{i,n})^2$, we assume $H(t)$ exists and is Lebesgue-almost surely

differentiable in $(0,T)$ *with derivative* H' *such that* $|H'(t_i) - \Delta_{i,n}/\Delta_n| \leq C\Delta_{i,n}$, *for any* t_i *in which* H *is differentiable, where* C *does not depend on* i *and* n.

Assumption 6. *The bandwidths* h_n, h'_n *are sequences of positive real numbers, such that, as* $n \to \infty$, $h_n \to 0$, $h'_n \to 0$, $nh_n \to \infty$, *and* $nh'_n \to \infty$. *The Kernel,* $K : \mathrm{R} \to \mathrm{R}_+$ *is any function with the properties:*

1. $K(x) = 0$ *for* $x > 0$;
2. K *is bounded and differentiable with bounded first derivative. Further,* $xK(x) \to 0$ *and* $xK'(x) \to 0$, *as* $x \to -\infty$;
3. $\int_{-\infty}^{0} K(x)\,dx = 1$ *and* $K_2 = \int_{-\infty}^{0} K^2(x)\,dx < \infty$.
4. K *has fast vanishing tail in the sense that for every positive sequence* $G_{n,t} \to \infty$, $\int_{-\infty}^{-G_{n,t}} K(x)dx \leq CG_{n,t}^{-B}$ *for some* $B > 0$ *and* $C > 0$;
5. $m_K(\alpha) = \int_{-\infty}^{0} K(x)\,|x|^{\alpha}\,dx < \infty$, *for all* $\alpha > -1$; $m'(\alpha) = \int_{-\infty}^{0} K^2(x)\,|x|^{\alpha}\,dx < \infty$, *for all* $\alpha > -1$.

A.2 Proofs of the main results

Proof of Theorem 2.1.

Denote by $\Delta_i Y = \sigma_{t_{i-1}} \Delta_i S$ the piecewise constant scale approximations of the increments $\Delta_i X$, $i = 1, 2, \ldots, n$, and consider the decomposition:

$$\sqrt{\frac{\Delta_n}{h_n}} \sum_{i=1}^{n} K\left(\frac{t_{i-1} - t}{h_n}\right) g\left(\frac{\Delta_i X}{\Delta_n^{1/\alpha}}\right) = A_n + E_n, \tag{30}$$

where A_n is the leading term based on the approximations:

$$A_n = \sqrt{\frac{\Delta_n}{h_n}} \sum_{i=1}^{n} K\left(\frac{t_{i-1} - t}{h_n}\right) g\left(\frac{\Delta_i Y}{\Delta_n^{1/\alpha}}\right), \tag{31}$$

and E_n is the approximation error of the form:

$$E_n = \sqrt{\frac{\Delta_n}{h_n}} \sum_{i=1}^{n} K\left(\frac{t_{i-1} - t}{h_n}\right) \left(g\left(\frac{\Delta_i X}{\Delta_n^{1/\alpha}}\right) - g\left(\frac{\Delta_i Y}{\Delta_n^{1/\alpha}}\right)\right). \tag{32}$$

The proof consists of showing that E_n is asymptotically negligible and $A_n \overset{stably}{\longrightarrow} \mathcal{N}\left(0, K_2\, \rho^{(\alpha)}_{\sigma_{t-}}\left(g^2\right)\right)$.

In order to prove the asymptotic negligibility of E_n it is enough to show that

$$\sum_{i=1}^{n} \mathbb{E}\left[|e_{n,i}| \mid \mathscr{F}_{i-1}\right] \xrightarrow{p} 0, \tag{33}$$

where $e_{n,i} = \sqrt{\frac{\Delta_n}{h_n}} K\left(\frac{t_{i-1}-t}{h_n}\right)\left(g\left(\frac{\Delta_i X}{\Delta_n^{1/\alpha}}\right) - g\left(\frac{\Delta_i Y}{\Delta_n^{1/\alpha}}\right)\right)$. Since $g(\cdot)$ is Lipschitz continuous, there exists a real constant $C > 0$ such that,

$$\left| g\left(\frac{\Delta_i X}{\Delta_n^{1/\alpha}}\right) - g\left(\frac{\Delta_i Y}{\Delta_n^{1/\alpha}}\right)\right| \leq C \left|\frac{\Delta_i X - \Delta_i Y}{\Delta_n^{1/\alpha}}\right|, \tag{34}$$

where

$$\Delta_i X - \Delta_i Y = \int_{t_{i-1}}^{t_i} \mu_s\, ds + \int_{t_{i-1}}^{t_i} \left(\sigma_s - \sigma_{t_{i-1}}\right)\, dS_s. \tag{35}$$

Combining inequality (34) with the algebraic inequality $|a+b| \leq |a| + |b|$ we obtain:

$$\sum_{i=1}^{n} \mathbb{E}\left[|e_{n,i}| \mid \mathscr{F}_{i-1}\right] \leq \sum_{i=1}^{n} \frac{\Delta_n^{\frac{\alpha-2}{2\alpha}}}{\sqrt{h_n}} K\left(\frac{t_{i-1}-t}{h_n}\right) \eta^n_{i,1} + \sum_{i=1}^{n} \frac{\Delta_n^{\frac{\alpha-2}{2\alpha}}}{\sqrt{h_n}} K\left(\frac{t_{i-1}-t}{h_n}\right) \eta^n_{i,2}, \tag{36}$$

where

$$\eta^n_{i,1} = \mathbb{E}\left[\int_{t_{i-1}}^{t_i} |\mu_s|\, ds \;\middle|\; \mathscr{F}_{i-1}\right], \quad \text{and} \quad \eta^n_{i,2} = \mathbb{E}\left[\left|\int_{t_{i-1}}^{t_i} \left(\sigma_s - \sigma_{t_{i-1}}\right)\, dS_s\right| \;\middle|\; \mathscr{F}_{i-1}\right]. \tag{37}$$

Since μ_t is bounded,

$$\eta^n_{i,1} = \mathbb{E}\left[\int_{t_{i-1}}^{t_i} |\mu_s|\, ds \;\middle|\; \mathscr{F}_{i-1}\right] \leq C\, \Delta_{n,i}. \tag{38}$$

Consequently,

$$\sum_{i=1}^{n} \frac{\Delta_n^{\frac{\alpha-2}{2\alpha}}}{\sqrt{h_n}} K\left(\frac{t_{i-1}-t}{h_n}\right) \eta^n_{i,1} = O_p\left(\sqrt{h_n}\, \Delta_n^{(\alpha-2)/2\alpha}\right). \tag{39}$$

Next, using the inner clock moment inequality of stable stochastic integrals (Rosinski and Woyczynski, 1985), for a constant $C > 0$, we obtain:

$$\eta^n_{i,2} \leq C\, \mathbb{E}\left[\left(\int_{t_{i-1}}^{t_i} \left|\sigma_s - \sigma_{t_{i-1}}\right|^{\alpha} ds\right)^{1/\alpha} \;\middle|\; \mathscr{F}_{i-1}\right]. \tag{40}$$

Since $\alpha > 1$,

$$\mathbb{E}\left[\left(\int_{t_{i-1}}^{t_i} \left|\sigma_s - \sigma_{t_{i-1}}\right|^{\alpha} ds\right)^{1/\alpha} \;\middle|\; \mathscr{F}_{i-1}\right] \leq \mathbb{E}\left[\int_{t_{i-1}}^{t_i} \left|\sigma_s - \sigma_{t_{i-1}}\right|\, ds \;\middle|\; \mathscr{F}_{i-1}\right], \tag{41}$$

where by Assumption 4 and Hölder inequality we have:

$$\mathbb{E}\left[\int_{t_{i-1}}^{t_i} \left|\sigma_s - \sigma_{t_{i-1}}\right| \, ds \;\middle|\; \mathscr{F}_{i-1}\right] = \int_{t_{i-1}}^{t_i} \mathbb{E}\left[\left|\sigma_s - \sigma_{t_{i-1}}\right| \mid \mathscr{F}_{i-1}\right] \, ds \leq C\, \Delta_{i,n}^{1+\Gamma/2}. \tag{42}$$

Consequently,

$$\sum_{i=1}^{n} \frac{\Delta_n^{\frac{\alpha-2}{2\alpha}}}{\sqrt{h_n}} K\left(\frac{t_{i-1}-t}{h_n}\right) \eta_{i,2}^n = O_p\left(\sqrt{h_n}\, \Delta_n^{\Gamma/2+(\alpha-2)/2\alpha}\right), \tag{43}$$

which implies that E_n is asymptotically negligible.

The leading term can be expressed as:

$$A_n = \sum_{i=1}^{n} \xi_i^n, \tag{44}$$

where

$$\xi_i^n = \sqrt{\frac{\Delta_n}{h_n}} K\left(\frac{t_{i-1}-t}{h_n}\right) g\left(\frac{\Delta_i Y}{\Delta_n^{1/\alpha}}\right). \tag{45}$$

Consequently, by Theorem 2.2.14 of Jacod and Protter (2012), to establish the convergence of A_n it is sufficient to verify the four conditions:

(i) $\sum_{i=1}^{n} \mathbb{E}\left[\xi_i^n \mid \mathscr{F}_{i-1}\right] \xrightarrow{p} 0$,

(ii) $\sum_{i=1}^{n} \mathbb{E}\left[\left(\xi_i^n\right)^2 \mid \mathscr{F}_{i-1}\right] \xrightarrow{p} K_2\, \rho_{\sigma_{t-}}^{(\alpha)}\left(g^2\right)$,

(iii) $\sum_{i=1}^{n} \mathbb{E}\left[\left(\xi_i^n\right)^4 \mid \mathscr{F}_{i-1}\right] \xrightarrow{p} 0$,

(iv) $\sum_{i=1}^{n} \mathbb{E}\left[\xi_i^n\, \Delta_i N \mid \mathscr{F}_{i-1}\right] \xrightarrow{p} 0$, where either $N = S$ or N is a martingale orthogonal to S.

Notice that the probability law of $\Delta_n^{-1/\alpha}\Delta_i Y$ is the same as the probability law of $\sigma_{t_{i-1}} S_1$, where S_1 is a standard symmetric stable variable. Thus, for every $r \geq 1$,

$$\mathbb{E}\left[g^r\left(\frac{\Delta_i Y}{\Delta_n^{1/\alpha}}\right) \;\middle|\; \mathscr{F}_{i-1}\right] = \rho_{\sigma_{t_{i-1}}}^{(\alpha)}\left(g^r\right), \tag{46}$$

with $\rho_{\sigma_{t_{i-1}}}^{(\alpha)}(g) = 0$ and $\left|\rho_{\sigma_{t_{i-1}}}^{(\alpha)}\left(g^r\right)\right| \leq C$ due to the properties of g. Consequently, the first condition (i) is fulfilled since $\mathbb{E}\left[\xi_i^n \mid \mathscr{F}_{i-1}\right] = 0$ by construction. For the second condition we have:

$$\mathbb{E}\left[\left(\xi_i^n\right)^2 \mid \mathscr{F}_{i-1}\right] = \frac{\Delta_n}{h_n} K^2\left(\frac{t_i - t}{h_n}\right) \mathbb{E}\left[g^2\left(\sigma_{t_{i-1}} S_1\right) \mid \mathscr{F}_{i-1}\right]. \tag{47}$$

Since $\mathbb{E}\left[g^2\left(\sigma_{t_{i-1}}S_1\right) \mid \mathscr{F}_{i-1}\right] = \rho^{(\alpha)}_{\sigma_{t_{i-1}}}\left(g^2\right)$, analogously to Mancini et al. (2015) we obtain:

$$\sum_{i=1}^{n} \frac{\Delta_n}{h_n} K^2\left(\frac{t_i - t}{h_n}\right) \mathbb{E}\left[g^2\left(\sigma_{t_{i-1}}S_1\right) \mid \mathscr{F}_{i-1}\right] \xrightarrow{p} K_2\, \rho^{(\alpha)}_{\sigma_{t-}}\left(g^2\right), \tag{48}$$

which proves that the second condition (ii) holds.

For the third condition, since g is bounded, we have:

$$\sum_{i=1}^{n} \mathbb{E}\left[(\xi_i^n)^4 \mid \mathscr{F}_{i-1}\right] \leq C \sum_{i=1}^{n} \frac{\Delta_n^2}{h_n^2} K^4\left(\frac{t_i - t}{h_n}\right) = O_p\left(\Delta_n\, h_n^{-1}\right), \tag{49}$$

which implies that the third condition (iii) holds.

Finally, since g is bounded, where exist nonrandom numbers $c_n \leq C_n$, such that $c_n \leq \xi_i^n \leq C_n$. Consequently, for any martingale N, we have:

$$\mathbb{E}\left[\xi_i^n\, \Delta_i N \mid \mathscr{F}_{i-1}\right] \leq C_n \mathbb{E}\left[\Delta_i N \mid \mathscr{F}_{i-1}\right] = 0, \tag{50}$$

and

$$\mathbb{E}\left[\xi_i^n\, \Delta_i N \mid \mathscr{F}_{i-1}\right] \geq c_n \mathbb{E}\left[\Delta_i N \mid \mathscr{F}_{i-1}\right] = 0, \tag{51}$$

implying that $\mathbb{E}\left[\xi_i^n\, \Delta_i N \mid \mathscr{F}_{i-1}\right] = 0$ and the fourth condition (iv) is fulfilled, which completes the proof.

□

Proof of Theorem 2.2.

Let $\nu_t = \rho^{(\alpha)}_{\sigma_{t-}}\left(g^2\right)$ and $\nu_t^n = \left(\widetilde{\sigma}_t^n\right)^2$. Then, by Theorem 2.1,

$$\sqrt{\frac{h_n}{\Delta_n\, K_2}}\, \widetilde{\mu}_t^n \xrightarrow{stably} \mathcal{N}\left(0, \nu_t\right). \tag{52}$$

Consequently, since the above convergence is stable, in order to complete the proof it is sufficient to show that

$$\nu_t^n \xrightarrow{p} \nu_t. \tag{53}$$

Recall that

$$\nu_t^n = \frac{\Delta_n}{h_n'} \sum_{i=1}^{n} K\left(\frac{t_{i-1} - t}{h_n'}\right) g^2\left(\frac{\Delta_i X}{\Delta_n^{1/\alpha}}\right). \tag{54}$$

It can be decomposed as

$$\nu_t^n = \frac{\Delta_n}{h'_n} \sum_{i=1}^{n} K\left(\frac{t_{i-1}-t}{h'_n}\right) g^2\left(\frac{\Delta_i Y}{\Delta_n^{1/\alpha}}\right) + E_n^\sigma, \tag{55}$$

where $\Delta_i Y$ are the approximations for the increments $\Delta_i X$ defined as in Theorem 2.1 and

$$E_n^\sigma = \frac{\Delta}{h'_n} \sum_{i=1}^{n} K\left(\frac{t_{i-1}-t}{h'_n}\right) \left(g^2\left(\frac{\Delta_i X}{\Delta_n^{1/\alpha}}\right) - g^2\left(\frac{\Delta_i Y}{\Delta_n^{1/\alpha}}\right)\right). \tag{56}$$

Since g is Lipschitz continuous, so is g^2. In particular, there exists a real constant $C > 0$ such that,

$$\left| g^2\left(\frac{\Delta_i X}{\Delta_n^{1/\alpha}}\right) - g^2\left(\frac{\Delta_i Y}{\Delta_n^{1/\alpha}}\right)\right| \leq C \left|\frac{\Delta_i X - \Delta_i Y}{\Delta_n^{1/\alpha}}\right|. \tag{57}$$

Consequently, analogously to the proof of the negligibility of E_n in Theorem 2.1 it follows that E_n^σ is asymptotically negligible.

It remains to prove that

$$\frac{\Delta_n}{h'_n} \sum_{i=1}^{n} K\left(\frac{t_{i-1}-t}{h'_n}\right) g^2\left(\frac{\Delta_i Y}{\Delta_n^{1/\alpha}}\right) \xrightarrow{p} \nu_t. \tag{58}$$

Analogously to the proof of the condition (ii) in Theorem 2.1 we immediately obtain:

$$\frac{\Delta_n}{h'_n} \sum_{i=1}^{n} K\left(\frac{t_{i-1}-t}{h'_n}\right) \mathbb{E}\left[g^2\left(\frac{\Delta_i Y}{\Delta_n^{1/\alpha}}\right) \,\middle|\, \mathscr{F}_{i-1}\right] \xrightarrow{p} \nu_t. \tag{59}$$

Next, consider the difference:

$$D_n = \frac{\Delta_n}{h'_n} \sum_{i=1}^{n} K\left(\frac{t_{i-1}-t}{h'_n}\right) g^2\left(\frac{\Delta_i Y}{\Delta_n^{1/\alpha}}\right) - \frac{\Delta_n}{h'_n} \sum_{i=1}^{n} K\left(\frac{t_{i-1}-t}{h'_n}\right) \mathbb{E}\left[g^2\left(\frac{\Delta_i Y}{\Delta_n^{1/\alpha}}\right) \,\middle|\, \mathscr{F}_{i-1}\right]. \tag{60}$$

It can be expressed as $D_n = \sum_{i=1}^{n} \eta_i^n$, where $\eta_i^n = \frac{\Delta_n}{h'_n} K\left(\frac{t_{i-1}-t}{h'_n}\right) \left(g^2\left(\frac{\Delta_i Y}{\Delta_n^{1/\alpha}}\right) - \mathbb{E}\left[g^2\left(\frac{\Delta_i Y}{\Delta_n^{1/\alpha}}\right) \,\middle|\, \mathscr{F}_{i-1}\right]\right)$. By construction, $\mathbb{E}\left[\eta_i^n \mid \mathscr{F}_{i-1}\right] = 0$. Since g^2 is bounded,

$$\sum_{i=1}^{n} \mathbb{E}\left[|\eta_i^n|^2 \mid \mathscr{F}_{i-1}\right] \leq C \sum_{i=1}^{n} \frac{\Delta_n^2}{(h'_n)^2} K^2\left(\frac{t_{i-1}-t}{h'_n}\right) = O_p\left(\frac{\Delta_n}{h'_n}\right), \tag{61}$$

which implies that D_n is asymptotically negligible and completes the proof. □

Proof of Theorem 2.3.

Set $\delta_n = (n/k_n)^{\frac{2-\alpha}{\alpha}}$. The proof consists of showing that, as $n \to \infty$,

(i) for some random variable $\overline{\nu}_t$,

$$\sqrt{\frac{\delta_n}{h_n}}\sum_{i=1}^{n-k_n+2} K\left(\frac{t_{i-1}-t}{h_n}\right) g\left(\frac{\Delta_{i-1}\overline{Z}}{(n/k_n)^{\frac{1}{\alpha}}}\right) \overset{stably}{\longrightarrow} \mathcal{N}\left(0,\overline{\nu}_t\right),$$

(ii)

$$\delta_n \left(\overline{\sigma}_t^n\right)^2 \overset{p}{\longrightarrow} \overline{\nu}_t.$$

Consider the decomposition:

$$\sqrt{\frac{\delta_n}{h_n}}\sum_{i=1}^{n-k_n+2} K\left(\frac{t_{i-1}-t}{h_n}\right) g\left(\frac{\Delta_{i-1}\overline{Z}}{(n/k_n)^{\frac{1}{\alpha}}}\right) = \overline{A}_n + \overline{E}_n, \tag{62}$$

where

$$\overline{A}_n = \sum_{i=1}^{n-k_n+2} \sqrt{\frac{\delta_n}{h_n}} K\left(\frac{t_{i-1}-t}{h_n}\right) g\left(\frac{\Delta_{i-1}\overline{u}}{(n/k_n)^{\frac{1}{\alpha}}}\right), \tag{63}$$

and

$$\overline{E}_n = \sum_{i=1}^{n-k_n+2} \sqrt{\frac{\delta_n}{h_n}} K\left(\frac{t_{i-1}-t}{h_n}\right) \left(g\left(\frac{\Delta_{i-1}\overline{Z}}{(n/k_n)^{\frac{1}{\alpha}}}\right) - g\left(\frac{\Delta_{i-1}\overline{u}}{(n/k_n)^{\frac{1}{\alpha}}}\right)\right). \tag{64}$$

The leading term is $\overline{A}_n$. Notice that the summands in $\overline{A}_n$ are zero-mean k_n-dependent with $k_n \to \infty$ due to the pre-averaging. Thus, analogously to the proof of the convergence of $M_{\epsilon,n}$ in Theorem 5 of Christensen et al. (2022) we conclude that

$$\overline{A}_n \overset{stably}{\longrightarrow} \mathcal{N}\left(0,\overline{\nu}_t\right), \tag{65}$$

for some random variable $\overline{\nu}_t$.

Thus, to complete the first part of the proof it remains to show that $\overline{E}_n$ is asymptotically negligible. Since $g(\cdot)$ is Lipschitz continuous, using the algebraic inequality $|a+b| \leq |a| + |b|$, for a real constant $C > 0$, we obtain:

$$\left|\overline{E}_n\right| \leq C \sum_{i=1}^{n-k_n+2} \sqrt{\frac{\delta_n}{h_n}} K\left(\frac{t_{i-1}-t}{h_n}\right) \left|\frac{\Delta_{i-1}\overline{X}}{(n/k_n)^{\frac{1}{\alpha}}}\right| \leq \overline{E}_{n,1} + \overline{E}_{n,2}, \tag{66}$$

where $\overline{E}_{n,1} = \sum_{i=1}^{n-k_n+2} \overline{\varepsilon}_i^{(1)}$ and $\overline{E}_{n,2} = \sum_{i=1}^{n-k_n+2} \overline{\varepsilon}_i^{(2)}$ with

$$\begin{aligned}
\overline{\varepsilon}_i^{(1)} &= C\sqrt{\frac{\delta_n}{h_n}} K\left(\frac{t_{i-1}-t}{h_n}\right) \left|\sum_{j=1}^{k_n-1} q_j^n \frac{\int_{t_{i+j-1}}^{t_{i+j}} \mu_s\, ds}{(n/k_n)^{\frac{1}{\alpha}}}\right|, \\
\overline{\varepsilon}_i^{(2)} &= C\sqrt{\frac{\delta_n}{h_n}} K\left(\frac{t_{i-1}-t}{h_n}\right) \left|\sum_{j=1}^{k_n-1} q_j^n \frac{\int_{t_{i+j-1}}^{t_{i+j}} \sigma_{s-}\, dS_s}{(n/k_n)^{\frac{1}{\alpha}}}\right|.
\end{aligned} \tag{67}$$

The random variables $\overline{\varepsilon}_i^{(k)}$, $k = 1, 2$, are $\mathscr{F}_{i+k_n-1}$-measurable. Consequently, to prove that $\overline{E}_{n,k}$ are asymptotically negligible it is sufficient to show that $k_n \sum_{i=1}^{n-k_n+2} \mathbb{E}\left[\overline{\varepsilon}_i^{(k)} \,\middle|\, \mathscr{F}_{i-1}\right] \xrightarrow{p} 0$.

Since μ_t is bounded,

$$\mathbb{E}\left[\int_{t_{i-1}}^{t_i} |\mu_s| \, ds \,\middle|\, \mathscr{F}_{i-1}\right] \leq C \, \Delta_{n,i} \leq C \, \frac{1}{n}. \tag{68}$$

Consequently, using the fact that $\left(\sum_{j=1}^{k_n-1} q_j^n \, \frac{1}{k_n}\right)$ converges to a constant, we obtain:

$$\begin{aligned} k_n \sum_{i=1}^{n-k_n+2} \mathbb{E}\left[\left|\overline{\varepsilon}_i^{(1)}\right| \,\middle|\, \mathscr{F}_{i-1}\right] &\leq C \sum_{i=1}^{n-k_n+2} k_n \sqrt{\frac{\delta_n}{h_n}} K\left(\frac{t_{i-1}-t}{h_n}\right) \left(\frac{n}{k_n}\right)^{-\frac{1}{\alpha}} \sum_{j=1}^{k_n-1} q_j^n \, \mathbb{E}\left[\int_{t_{i+j-1}}^{t_{i+j}} |\mu_s| \, ds \,\middle|\, \mathscr{F}_{i-1}\right] \\ &\leq C \sum_{i=1}^{n-k_n+2} k_n \sqrt{\frac{\delta_n}{h_n}} K\left(\frac{t_{i-1}-t}{h_n}\right) \left(\frac{n}{k_n}\right)^{-\frac{1}{\alpha}} \frac{k_n}{n} \left(\sum_{j=1}^{k_n-1} q_j^n \, \frac{1}{k_n}\right) \\ &\sim \sqrt{\frac{h_n k_n^5}{n}} \longrightarrow 0, \end{aligned} \tag{69}$$

which implies that $\overline{E}_{n,1}$ is asymptotically negligible.

Next, since σ_t is bounded and by the properties of α-stable motion, we have:

$$\mathbb{E}\left[\left|\int_{t_{i-1}}^{t_i} \sigma_s \, dS_s\right| \,\middle|\, \mathscr{F}_{i-1}\right] \leq C \, \Delta_{n,i}^{1/\alpha} \leq C \, \left(\frac{1}{n}\right)^{1/\alpha}. \tag{70}$$

Consequently,

$$\begin{aligned} k_n \sum_{i=1}^{n-k_n+2} \mathbb{E}\left[\left|\overline{\varepsilon}_i^{(2)}\right| \,\middle|\, \mathscr{F}_{i-1}\right] &\leq C \sum_{i=1}^{n-k_n+2} k_n \sqrt{\frac{\delta_n}{h_n}} K\left(\frac{t_{i-1}-t}{h_n}\right) \left(\frac{n}{k_n}\right)^{-\frac{1}{\alpha}} \sum_{j=1}^{k_n-1} q_j^n \, \mathbb{E}\left[\left|\int_{t_{i+j-1}}^{t_{i+j}} \sigma_s \, dS_s\right| \,\middle|\, \mathscr{F}_{i-1}\right] \\ &\leq C \sum_{i=1}^{n-k_n+2} k_n \sqrt{\frac{\delta_n}{h_n}} K\left(\frac{t_{i-1}-t}{h_n}\right) \left(\frac{n}{k_n}\right)^{-\frac{1}{\alpha}} \frac{k_n}{n^{1/\alpha}} \left(\sum_{j=1}^{k_n-1} q_j^n \, \frac{1}{k_n}\right) \\ &\sim \sqrt{\frac{h_n k_n^5}{n^{\frac{2-\alpha}{\alpha}}}} \longrightarrow 0, \end{aligned} \tag{71}$$

which implies that $\overline{E}_{n,2}$ is asymptotically negligible.

The second part of the proof, namely the convergence $\delta_n \left(\overline{\sigma}_t^n\right)^2 \xrightarrow{p} \overline{\nu}_t$ follow from the same arguments as the convergence of the HAC estimator in Theorem 5 of Christensen et al. (2022), which completes the proof.

□